JACS
JOURNAL OF THE AMERICAN CHEMICAL SOCIETY

Article

pubs.acs.org/JACS

A Label-Free, Electrochemical SERS-Based Assay for Detection of DNA Hybridization and Discrimination of Mutations

Robert P. Johnson, James A. Richardson, Tom Brown, and Philip N. Bartlett*

School of Chemistry, University of Southampton, Southampton SO17 1BJ, United Kingdom

Supporting Information

ABSTRACT: A label-free, surface-enhanced Raman spectroscopy-based assay for detecting DNA hybridization at an electrode surface and for distinguishing between mutations in DNA is demonstrated. Surface-immobilized DNA is exposed to a binding agent that is selective for dsDNA and acts as a reporter molecule. Upon application of a negative potential, the dsDNA denatures into its constituent strands, and the changes in the spectra of the reporter molecule are monitored. This method has been used to distinguish between a wild-type, 1653C/T single-point mutation and ΔF508 triplet deletion in the CFTR gene. The use of dsDNA-selective binding agents as reporter molecules in a discrimination assay removes the burden of synthetically modifying the target to be detected, while retaining flexibility in the choice of the reporter molecule.

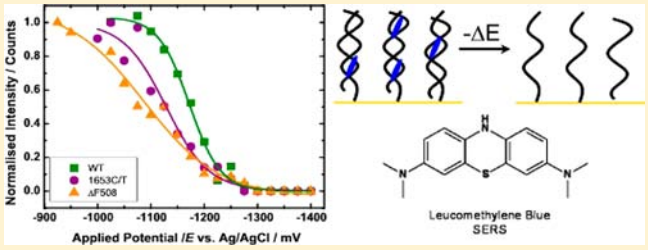

INTRODUCTION

Mutations in DNA are the cause of a wide range of genetic diseases, including cystic fibrosis.[1] Typically, mutations in DNA sequences are identified through differential denaturation, in which differences in structural stability are identified by thermally melting a sequence of interest and determining the melting temperature. Differential denaturation experiments also form a key aspect of forensic assays, where short tandem repeats (STRs) are used in DNA fingerprinting, and in the emerging field of pharmacogenetics, where patients who have a genetically pre-disposed risk of adverse side effects to certain medications can be identified.[2]

Many existing DNA discrimination assays exploit the use of a synthetically attached label group that is used to detect hybridization and/or follow DNA denaturation. However, this methodology often makes the technology inherently challenging to integrate into a device that could be used at the point of care. This is a common problem with many DNA detection and discrimination assays, where the time, difficulty, and expense of synthetically pre-treating a target analyte greatly diminish their effectiveness.[3] To this end, there has been a growing interest in "label-free detection", that is, the detection and discrimination of DNA without the requirement to synthetically pre-treat the DNA to be detected prior to analysis.

Several groups have reported label-free methods for detecting DNA in recent years, including the use of carbon nanotube network field-effect transistors,[4,5] fluorescent methodologies,[6−9] nanomechanical cantilevers,[10] quartz crystal microbalance measurements,[11] and surface plasmon resonance.[12,13] Halas and co-workers demonstrated the label-free detection of DNA with surface-enhanced Raman spectroscopy (SERS) by substitution of adenine in a surface-immobilized probe sequence with 2-aminopurine.[14] Electrochemical methods have been used extensively in DNA detection assays, as summarized in recent review articles.[15,16] In particular, label-free detection using impedance spectroscopy has received much attention,[17−19] but the sensitivity of impendence measurements to small changes in environmental conditions leaves the reproducibility and reliability of this method open to debate.

While a wide variety of label-free biosensors have been demonstrated for the detection of DNA, there are fewer that are capable of actually discriminating between mutations. Nasef et al. demonstrated that differential pulse voltammetry can be combined with thermal denaturation of DNA to discriminate between a perfectly complementary and mutated target oligonucleotide that is non-covalently bound to methylene blue.[20] Electric field-induced denaturation, combined with either fluorescence[21] or surface plasmon resonance,[22] has also been employed for discriminating between mutations, while a recent report by Bell et al. demonstrated that single-base mismatches can be detected directly from unlabeled and unmodified oligonucleotides by utilizing silver colloid SERS substrates.[23] In all of these methods, a specific single mutation was discriminated from a perfectly complementary base-pair, and thus none demonstrates the flexibility of conventional denaturation experiments that can be performed in a laboratory, which can differentiate a wide range of targets on the basis of stability.

Previously, we demonstrated that electrochemically driven DNA denaturation can be combined with SERS monitoring to distinguish DNA duplexes on the basis of their structural stability.[24−28] In a typical SERS electrochemical melting assay, a modified probe strand is first attached to the gold SERS

Received: May 14, 2012
Published: July 26, 2012

dx.doi.org/10.1021/ja304663t | J. Am. Chem. Soc. 2012, 134, 14099−14107

substrate via a series of three dithiol linkers at a coverage of around 1.5×10^{12} molecules cm^{-2} to ensure that hybridization with DNA from solution is not sterically hindered.[29,30] The surface is then passivated by treatment with mercaptohexanol. This prevents the non-specific adsorption of DNA at the gold surface[29,30] and re-orients the probes to stand out from the surface.[31,32] The target DNA strands to be analyzed are synthetically labeled with a dye molecule (such as Cy3 or Texas Red), introduced from solution, and allowed to hybridize to the bound probe strand to form dsDNA at the surface. The potential is swept negative, and the attenuation of the signal due to the denaturation and subsequent diffusion of the target strand away from the surface is used to construct a melting curve that has a mid-point that is dependent on the stability of the immobilized DNA. This methodology has been successfully applied to demonstrate the characterization of mutations in the gene responsible for coding for the Cystic Fibrosis Transmembrane Regulator (CFTR) protein through discrimination of the wild-type, 1653C/T SNP, and ΔF508 triplet deletion using spectra recorded from the 0.02 attomole level (12 000 molecules) of surface-bound dsDNA.[26] The same approach has also been used to discriminate STR sequences as used in DNA fingerprinting at a similar level and through measurements on DNA produced by asymmetric PCR without the need for a subsequent purification step.[24]

In this contribution, we demonstrate the first use of DNA binding agents as a method for selectively detecting dsDNA at a SERS substrate without prior synthetic modification of the target to be detected. The use of binding agents is simple and effective, removing the need for complex nucleic acid modification,[14] and does not have the detectable target limitations of other label-free SERS-based approaches.[23] We also demonstrate for the first time that SERS can be used to elucidate the mechanism through which a binding agent interacts with the immobilized dsDNA by applying the surface selection rule for Raman spectroscopy. In this approach, any binding agents in the bulk solution do not contribute to the observed SER spectra because of the strong surface selectivity of the enhancement. Further, existing methods for determining molecule−DNA binding mechanisms, such as X-ray diffraction and circular chroism, are unsuitable for studying DNA immobilized to surfaces. Finally, by combining label-free detection with the electrochemical denaturation methods developed in our earlier work,[26] we demonstrate a label-free assay capable of discriminating between mutations in the CFTR gene. Since electrochemical melting discriminates between sequences on the basis of the stability of the duplex, we anticipate that the label-free method described here can be applied to a wide range of targets of interest, and thus demonstrates significant future potential for integration into a point-of-care device.

EXPERIMENTAL SECTION

All reagents used were analytical grade and obtained from Sigma-Aldrich, unless stated otherwise.

Fabrication of Sphere Segment Void (SSV) Substrates. SER-active nanovoid substrates were formed using a templated electrodeposition process described previously by our group. Typically, a standard gold−chrome-coated microscope slide is prepared by thermal vapor deposition of a 10 nm chromium adhesion layer followed by approximately 200 nm gold onto a standard glass microscope slide (76 mm × 26 mm × 1 mm). The gold−chrome-coated slide is cut into eight pieces (19 mm × 13 mm) and each piece cleaned by sonication in ethanol (Sigma, HPLC). The monolayer template was produced by a capillary force method utilizing polystyrene spheres (Fisher Scientific as a 1 wt % aqueous suspension) to leave a well-ordered hexagonal array of spheres on the gold-coated glass slide. Gold was deposited through the template at −0.72 V vs SCE from a commercial cyanide-free gold plating solution (Metalor, ECF 60) containing an additive (Metalor, Brightener E3) to leave a bright and smooth finish. Following electrodeposition, the polystyrene spheres were removed by dissolving in dimethylformamide (Rathburn, HPLC), and the substrates were rinsed thoroughly with water. In this work, 600 nm spheres were used, and the deposition height was 480 nm.

Oligonucleotide Synthesis. Standard DNA phosphoramidites, solid supports, and additional reagents were purchased from Link Technologies, Sigma, and Applied Biosystems. Dithiol phosphoramidite was purchased from Glen Research. All oligonucleotides were synthesized on an Applied Biosystems 394 automated DNA/RNA synthesizer using standard 0.2 or 1.0 μmol phosphoramidite cycles of acid-catalyzed detritylation, coupling, capping, and iodine oxidation. Stepwise coupling efficiencies and overall yields were determined by the automated trityl cation conductivity monitoring facility and in all cases were >98.0%. All β-cyanoethyl phosphoramidite monomers were dissolved in anhydrous acetonitrile to a concentration of 0.1 M immediately prior to use. The coupling time for normal (A, G, C, T) monomers was 35 s, and the coupling time for the dithiol monomers was extended to 600 s. Cleavage of oligonucleotides from the solid support and de-protection were achieved by exposure to concentrated aqueous ammonia for 60 min at room temperature, followed by heating in a sealed tube for 5 h at 55 °C.

Reversed-phase HPLC purification was carried out on a Gilson system using a Phenomenex column (C8), 10 mm × 250 mm, pore size 100 Å.

The following HPLC conditions were used: run time 20 min, flow rate 4 mL min^{-1}, binary system, gradient: time in min (% buffer B) 0 (0), 3 (0), 3.5 (15), 15 (60), 16 (100), 17 (100), 17.5 (0), 20 (0); elution buffer A, 0.1 M ammonium acetate, pH 7.0; buffer B, 0.1 M ammonium acetate with 50% acetonitrile, pH 7.0. Elution of oligonucleotides was monitored by ultraviolet absorption at 295 nm. After HPLC purification, oligonucleotides were de-salted using NAP-10 Sephadex columns (GE Healthcare), aliquoted into Eppendorf tubes, and stored at −20 °C. All oligonucleotides were characterized by MALDI-TOF mass spectrometry and capillary electrophoresis. The sequences utilized in this study are listed in Table 1.

Table 1. Sequences of the Probe and Target Oligonucleotides Used in This Study[a]

probe	5′ AGGAAACACCAAAGATGATATT 3′
wild -type	3′ TCCTTTGTGGTTTCTACTATAA 5′
1653C/T SNP	3′ TCCTTTGTGGTTT**T**TACTATAA 5′
ΔF508 deletion	3′ TCCTTTGTGG---CTACTATAA 5′

[a]Mutations in the 1653C/T single nucleotide polymorphism (SNP) and ΔF508 triple deletion oligonucleotides are highlighted in boldface. The probe strand was modified at the 5′ end with a dithiol linker as shown in Figure 1.

Substrates were immersed into a 10 mM Tris buffer (pH 7.2) containing 1 M NaCl and 1 μM of the dithiol-modified DNA strand (the probe strand) for 48 h, yielding a monolayer with approximately 1% coverage.[27] The thiol anchor was specifically designed with hexaethyleneglycol groups (Figure 1) that provide a large molecular footprint. This maximizes the efficiency of hybridization upon introduction of a target nucleic acid by preventing steric hindrance. Furthermore, the formation of six sulfur−gold bonds for each oligonucleotide probe significantly increases the stability of the DNA−gold conjugate,[33,34] preventing reductive desorption during electrochemical melting, and permits the same substrate to be re-used for multiple experiments if desired.[35]

The remaining surface was then passivated by immersing the substrate into a mixture of mercaptohexanol (1 mM). As reported previously, mercaptohexanol forms a dense sub-layer that prevents

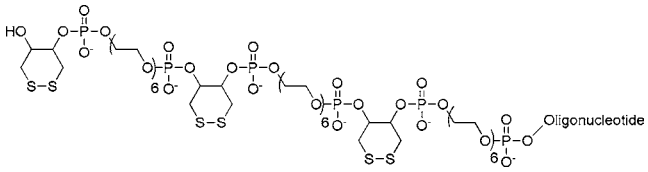

Figure 1. Structure of the disulfide (surface attachment) linker, specifically designed with hexaethyleneglycol groups to provide a large molecular footprint, and with six sulfur groups for enhanced stability.

non-specific binding[29,30] and forces the bound DNA strands into an upright conformation.[31,32] Substrates were rinsed with 10 mM Tris buffer (pH 7.2) containing 0.1 M NaCl several times before use in electrochemical melting experiments.

Electrochemical Melting Procedure. Electrochemical melting experiments were carried out in a custom-built spectro-electrochemical Raman cell (Ventacon Ltd.) specifically designed for use with a Renishaw 2000 Raman microscope. It utilizes a horizontal geometry for viewing under the microscope, maintaining a thin 150 μL liquid film on the substrate. Electrochemical control is provided by a three-electrode arrangement inside the cell, where the substrate is used as the working electrode, a platinum wire as the counter, and silver/silver chloride as the reference. In a typical electrochemical melting experiment, the potential was swept at 0.5 mV s^{-1} from a starting potential of −0.2 to −1.6 V in 10 mM Tris buffer containing 1 M NaCl. All electrochemical measurements were carried out using an EcoChemie μAutolabIII potentiostat/galvanostat at room temperature.

Raman Instrumentation. Raman spectra were acquired using a 50× objective on a Renishaw 2000 microscope instrument equipped with a 632.8 nm He−Ne laser and Prior XYZ stage controller. The diameter of the laser spot was 1 μm. Typically, Raman spectra were acquired from a 10 × 10 μm area with the laser moved approximately 2 μm between measurements in order to avoid bleaching effects. Various acquisition parameters were used; these are reported with the data in the Results section.

Data Analysis. SERS spectra presented were baseline-corrected using a polynomial multipoint fitting function, and curve-fitting was performed as required with Renishaw WiRe 3.1. The Raman intensities of the peaks are taken as height above the baseline. A Boltzmann function was used to fit sigmoidal curves to the melting profiles (Origin 8.6), and the first derivative of the fits was used to determine the melting points (mid-points of the melting curves).

RESULTS AND DISCUSSION

Choice of DNA Binding Agent. We have demonstrated previously that the denaturation of dsDNA at an electrode surface upon application of a negative potential can be monitored by the changes in SERS signal from a label covalently attached to the target strand. Typical labels used are the fluorophores Texas Red, Cy3, and Cy5, but many more labels that could potentially be used are commercially available. The success of a label-free SERS-based assay for detecting dsDNA at a surface and discriminating between mutations requires maintaining the flexibility of the reporter molecule while at the same time eliminating the need for a synthetic pretreatment of the target to be detected prior to analysis.

A range of small dye molecules, such as methylene blue and DAPI (see Figure 2), can bind to DNA. Typically, these molecules bind by electrostatic interactions, intercalation, or a minor-groove interaction.[36] To successfully utilize a DNA binding agent for a SERS detection and discrimination assay, the binding agent chosen must be selective for dsDNA; therefore, molecules that bind exclusively via electrostatic interactions with DNA were not considered.

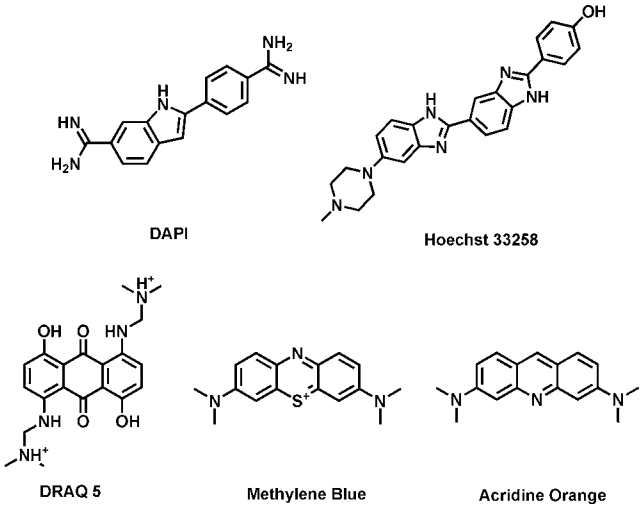

Figure 2. Structures of the five DNA binding agents used.

The Raman surface selection rule states that those bands in the spectra that are most intense will be associated with a vibrational mode that has a component of the polarizability tensor in a direction perpendicular to the surface.[37,38] Weaker contributions to the spectra will come from vibrational modes that have a polarizability tensor parallel to the surface. Intercalative agents typically bind parallel to and in between the base-pairs of DNA, and will theoretically provide weak spectra because the strongest vibrational modes (i.e., those from the aromatic rings) will be parallel to the surface when the dsDNA strands are orientated perpendicular to the surface. In contrast, molecules in the minor groove, which is nearly perpendicular to the base-pairs, will provide strong spectra because the strongest vibrational modes will be perpendicular to the surface.

In total, five binding agents were screened for utilization in a SERS detection and discrimination assay, and their structures are shown in Figure 2. Both intercalators and minor-groove binders were screened as potential binding agents. While minor-groove binders theoretically better suit the criteria for strong spectral intensity as described in the preceding paragraphs, most intercalators have at least some vibrational modes that lie perpendicular to the base-pairs between which they are situated, and these vibrational modes should easily be detectable. Two of the dyes chosen were resonant with the pump laser (633 nm HeNe) used to collect the SERS spectra, and it was anticipated that this would provide an additional resonant Raman effect (approximately 10^3 over and above SERS) and increase the sensitivity of detection. The properties of the five binding agents studied are shown in Table 2.

Label-Free Detection of dsDNA at an SSV Surface. SSV substrates with immobilized dsDNA were prepared as described in the Experimental Section. Following hybridization of the target strand, substrates were exposed to a 1 mM solution of

Table 2. Properties of the Five DNA Binding Agents Used

binding agent	binding mode	λ_{Ex} (nm)	λ_{Em} (nm)
acridine orange	intercalation[39]	502	525
DRAQ 5	intercalation[40]	647	670
Hoechst 33258	minor groove[41,42]	352	461
DAPI	minor groove[41,42]	358	461
methylene blue	multiple[39,43,44]	664	682

dx.doi.org/10.1021/ja304663t | J. Am. Chem. Soc. 2012, 134, 14099−14107

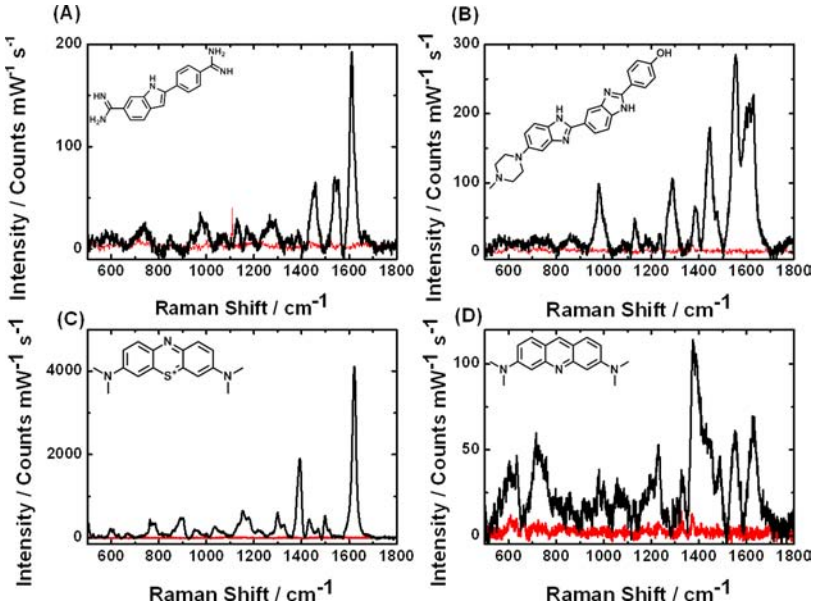

Figure 3. Detection of DNA hybridization at an SSV surface by using dsDNA-selective binding agents. (A) DAPI, (B) Hoechst 33258, (C) methylene blue, and (D) acridine orange in the presence of surface-immobilized single-stranded (red line) and double-stranded (black line) DNA. Spectra were collected in extended mode using two averaged acquisitions. Collection times have been normalized and spectra have been background subtracted for clarity and ease of comparison.

the chosen DNA binding agent for 3 h. Substrates were then rinsed thoroughly with a 10 mM Tris buffer solution (pH 7.2) containing 1 M NaCl before measurement to remove any weakly interacting or excess binding agents. Rinsing ensures that the SERS spectra are acquired only from those binding agents that are strongly bound to the surface-immobilized dsDNA.

It was possible to detect dsDNA immobilized at an SSV substrate with four of the five binding agents studied. Acquisition of SER spectra at an SSV surface in the presence of the fluorescent label DRAQ-5 resulted in immediate saturation of the detector during measurement, even when very short acquisition times (<5 s) and low laser powers (<1 mW) were used. This suggests that while DRAQ 5 intercalates successfully into surface-immobilized dsDNA, the strong fluorescence of this molecule makes SERS detection impossible with a 633 nm excitation source. The SER(R)S spectra of Hoechst 33258, DAPI, methylene blue, and acridine orange in the presence of surface-immobilized single-stranded (ss) and double-stranded (ds) DNA are shown in Figure 3.

DAPI, Hoechst 33258, acridine orange, and methylene blue were found to be completely selective for dsDNA in our detection assay (compare the black and red spectra in Figure 3). While these molecules sometimes find use in ssDNA staining protocols,[45] the interaction between the binding agent and the ssDNA is typically weak and only electrostatic in nature. Prior to measurement, substrates were rinsed thoroughly in a 10 mM Tris buffer (pH 7.2) containing 1 M NaCl. The large quantity of ions in solution screens the electrostatic interactions between the binding agent and the ssDNA, and any molecules bound through a weak electrostatic interaction are washed away from the surface.

Stronger intercalation and groove-binding interactions can occur only in dsDNA. Furthermore, ssDNA immobilized at a surface is significantly less accessible than in solution, particularly at high salt concentrations and at room temperature, where recent studies by Rant et al. suggest that it adopts a compressed orientation close to the electrode surface, with little extension out into the solution.[46]

In our earlier work, we demonstrated that the labels Texas Red and Cy5 covalently attached to target DNA were effective reporter molecules in a SERS-based discrimination assay with a 633 nm excitation source, despite their intense fluorescence in solution.[26] In this case the label is attached proximal to the surface of the SERS substrate, and the majority of the fluorescence is quenched. Since the position at which DRAQ-5 intercalates into the immobilized dsDNA cannot be reliably controlled, any metal−fluorophore quenching is not as effective.

The same problem did not occur with methylene blue, which despite its use as a fluorescent stain produced very intense Raman spectra. The spectrum of this molecule was found to be significantly more intense than that observed for DAPI, Hoechst 33258, or acridine orange due to resonance excitation by the 633 nm laser (note the difference in vertical scales in Figure 3). This resonance Raman effect gives rise to $\sim 10^3$ enhancement, creating a $\sim 10^9$ enhancement overall when combined with SERS for those bands strongly associated with the resonant chromophore of the molecule.[47]

The minor-groove binders DAPI and Hoechst 33258 have been shown to bind to repeating AT tracks and are highly selective for dsDNA.[41,42] For the oligonucleotides used in this study, the AT repeat region is at the 3′ end of the probe strand and at the 5′ end of the target strand. In our assay, where the probe strand is attached to the gold substrate through a thiol anchor at the 5′ end, it is reasonable to assume that these binding agents are held in the minor groove approximately 20 base-pairs (9 nm) from the surface. Previously, we have shown that the surface coverage of these oligonucleotides immobilized at an SSV surface is roughly 1×10^{12} molecules cm^{-2}, and assuming that one molecule of DAPI or Hoechst binds to each dsDNA molecule, the SERS spectra would correspond to approximately 12 500 molecules. This demonstrates the outstanding capabilities of the SSV substrate, where it is

possible to detect molecules at the attomole level even when the conditions are not optimal. In this case, the molecule to be detected is not resonant with the excitation source and is far from the metal−dielectric boundary, where the enhancement by the surface plasmon mode is most intense.

The detection of multiple binding agents also highlights the flexibility of our label-free SERS detection assay. While resonant methylene blue proved the best choice for use as reporter molecules with the 633 nm excitation laser used in our study, it should be possible to obtain the resonant SERS effect from other DNA binding agents by utilizing another excitation wavelength. For example, Hoechst 33258 and DAPI would be resonant with a UV (363 nm) laser. In the future, it should be possible to design and synthesize dsDNA-selective binding agents to be resonant at a chosen wavelength. Of particular interest would be a binding agent resonant at 785 nm, as diode lasers at this wavelength are portable and low cost and can easily be integrated into small point-of-care devices.

Elucidation of Binding Mechanism. While the SER(R)S spectra of methylene blue, Hoechst 33258, and DAPI were in good agreement with those reported previously, the spectrum of acridine orange bound to immobilized dsDNA showed significant differences in comparison to the previously reported SER spectra,[48] with only some of the expected peaks present. This can be explained by considering the Raman surface selection rule[37,38] and the orientation of the acridine orange with respect to the SSV surface.

The Raman surface selection rule states that those bands in the spectra that are most intense will be associated with a vibrational mode that has a component of the polarizability tensor in a direction perpendicular to the surface.[37,38] Weaker contributions to the spectra will come from vibrational modes that have the components of the polarizability tensor parallel to the surface.

Since the binding mechanism of acridine orange to dsDNA is exclusively intercalation,[39,49] in our assay the molecule will lie in a position parallel to the SSV surface. In this orientation, the vibrational modes with large polarizability components perpendicular to the surface will typically be deformations of the methyl groups that lie out-of-plane with the aromatic ring. Conversely, when acridine orange is perpendicular to the SERS surface, as described in the study by Zimmerman et al.,[48] the vibrational modes with large polarizability components perpendicular to the surface will be stretches of the aromatic ring.

The orientation of acridine orange with respect to the surface was confirmed by a further experiment. A 1 mM acridine orange solution was dropped onto an SSV substrate and allowed to dry. It was envisaged that this would provide an ensemble of random molecular orientations at the surface. The SERS spectrum of dsDNA-bound acridine orange (in a fixed orientation) was compared with the SERS spectrum of acridine orange in random orientations (Figure 4).

The spectrum of the drop-coated acridine orange layer is in good agreement with previous literature reports, and peaks were assigned on the basis of a very detailed study by Zimmerman et al.[48] Comparison of the drop-coated spectrum with that for acridine orange bound to surface-immobilized dsDNA shown in Figure 4 demonstrates the Raman surface selection rule and highlights how SERS can be used to determine the mechanism and orientation with which small molecules bind to dsDNA. From this result it can be deduced that acridine orange binds to dsDNA exclusively through

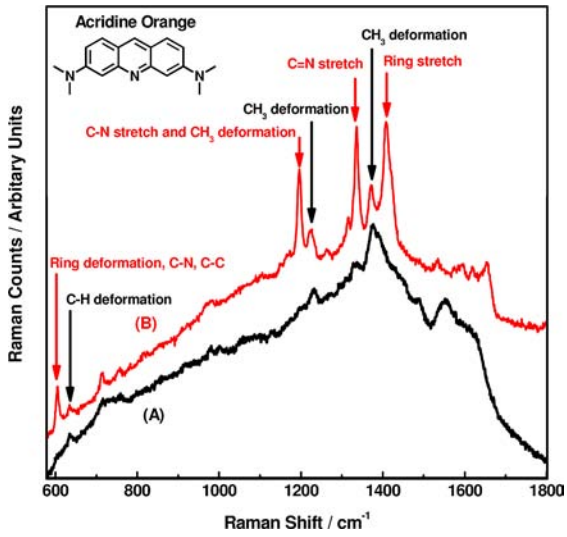

Figure 4. Elucidation of the binding mode of acridine orange bound to surface-immobilized dsDNA. SERS spectra of acridine orange (A, black line) bound to dsDNA and held in a fixed orientation parallel to an SSV surface and (B, red line) in an ensemble of orientations dried at an SSV surface. Spectra were collected with (A) 2 × 45 s and (B) 1 × 10 s acquisition and are presented without further correction for clarity. Peak assignments are based on those reported by Zimmerman et al.[48]

intercalation, which is consistent with literature reports for this molecule.[39,49]

Both DAPI and Hoechst 33258 are reported to bind to dsDNA mainly through minor-groove interactions[50−53] and are therefore expected to have an orientation nearly perpendicular to the substrate surface. The SERS spectra presented in Figure 3 are consistent with this because none of the expected bands from the aromatic backbone are absent, as would be the case if this part of the molecule were parallel to the metal surface. Indeed, the spectra are in good agreement with previous literature reports in which the binding orientation of the aromatic backbone with respect to the surface is random (in the case of DAPI,[54] where all bands are expected to be observed) or perpendicular (in the case of methylene blue and Hoechst 33258,[55,56] where all the bands in the plane of the aromatic backbone are expected to be observed).

The exact mode of methylene blue binding to dsDNA has been the subject of extensive research, particularly in computational simulations, which have shown that it is sequence dependent.[39,43,44] The mode of methylene blue binding also appears to be related to ionic strength, with evidence suggesting that intercalation is stabilized and favored at low salt concentrations.[44,57] In our assay, the ionic strength of the buffer is 1 M, and based on this intercalation is less likely. In addition to intercalation and minor-groove interactions, there is some evidence to suggest that methylene blue can interact directly with guanine bases,[58,59] but these are not specific to dsDNA, and results for ssDNA shown in Figure 3c show that methylene blue bound to DNA through this mechanism can be washed away through rinsing in high ionic strength buffer.

For AT-rich sequences, minor-groove binding is believed to be favored over intercalation.[43] In the case of the sequences used in this study, the AT content (that is, the percentage of AT base-pairs) is >70%, and it can be assumed that the majority of the methylene blue is bound via a minor-groove interaction in the surface-immobilized dsDNA used in this study. The

dx.doi.org/10.1021/ja304663t | J. Am. Chem. Soc. 2012, 134, 14099−14107

SERS spectrum for methylene blue bound to dsDNA at an SSV substrate presented in Figure 4 is consistent with this because the aromatic C═C and C═N ring stretches are very intense, which would not be the case if the methylene blue were bound exclusively through intercalation.[57−59]

Label-Free Discrimination of Mutations. Methylene blue is a relatively non-toxic dsDNA binding agent that is resonant with 633 nm excitation and as such is an ideal candidate for initial label-free SERS electrochemical melting experiments. However, its use as a reporter molecule in an electrochemical melting assay was found to be complicated because it is readily reduced at negative potentials to its colorless leuco form, which is not resonant with the 633 nm excitation wavelength and has a slightly different structure (Figure 5). Using SER(R)S, it is possible to monitor the reduction and oxidation of methylene blue while it is bound to the minor groove of surface-immobilized dsDNA.

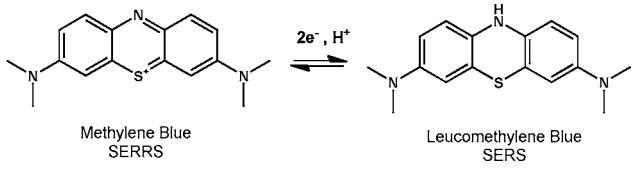

Figure 5. Diagram illustrating the structural changes that occur when methylene blue is electrochemically reduced to leucomethylene blue.

SERRS can effectively be turned on or off by switching the molecule between its resonant and non-resonant forms (Figure 5). The transformation of methylene blue to leucomethylene blue can be observed from the band at 1622 cm^{-1} and the broad spectral feature at 1388 cm^{-1} (Figure 6).

As the methylene blue is gradually reduced, both features at 1622 and 1388 cm^{-1} drop rapidly in intensity due to the loss of resonance with the excitation wavelength. Eventually, the 1622 cm^{-1} band is lost completely, while the 1388 cm^{-1} feature remains. While the band at 1622 cm^{-1} is typically assigned to a C═C ring stretch in literature reports,[60−62] the results presented in Figure 6 suggest that a C═N ring stretch is a more suitable assignment because of the reversible disappearance of the peak as the potential is swept negative and the methylene blue is reduced to leucomethylene blue. Upon reversing the potential, this C═N band re-appears, and the overall intensity of the spectra increases as the leucomethylene blue is oxidized back to methylene blue and the resonance of the molecule with the excitation wavelength is restored. The full recovery of the methylene blue SERR spectrum on the reverse scan demonstrates that the leucomethylene blue remains associated with the dsDNA, in contrast to some previous reports that suggest that the redox probe dissociates readily from dsDNA after reduction to leucomethylene blue.[63,64]

The peak intensities of the bands at 1450, 1622, 1390, and 1372 cm^{-1} for the methylene blue/leucomethylene blue were monitored as a function of applied potential during a SERS melting experiment in which the potential was swept between −100 and −1400 mV vs Ag/AgCl (Figure 7). The broad spectral feature at 1388 cm^{-1} is the most challenging to assign and is likely a convolution of two peaks. We attempted to fit the spectral feature to two overlapping Gaussian bands centered at 1372 and 1390 cm^{-1} (see Supporting Information). We postulate that the first peak, centered at 1372 cm^{-1}, is from a C═C aromatic ring stretch, present in both methylene blue

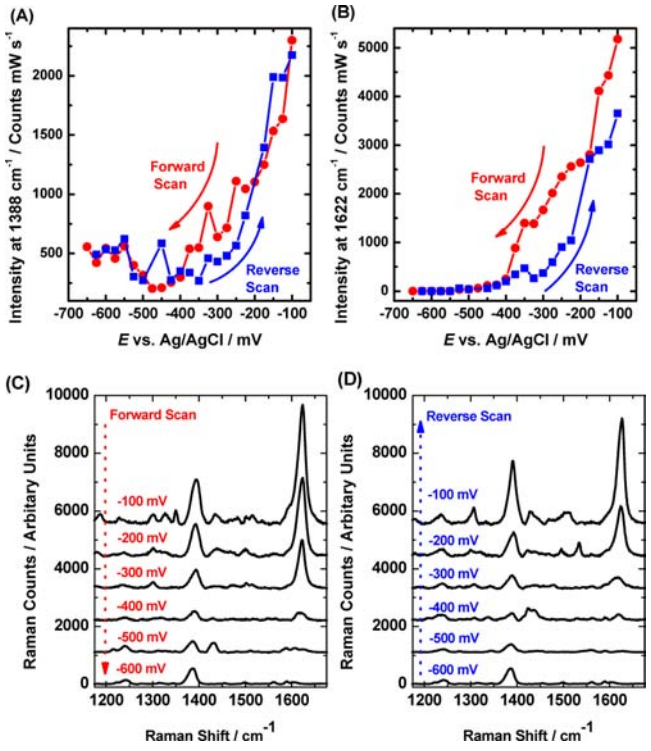

Figure 6. Monitoring the reduction and oxidation of methylene blue bound to the minor groove of surface-immobilized dsDNA. Changes in the peak height of (A) the feature at 1580 cm^{-1} and (B) the C═N stretch at 1622 cm^{-1} as a function of applied potential, and representative spectra illustrating this change during the (C) forward and (D) reverse scan of a cyclic voltammetry experiment in which the potential at the electrode surface was swept at 0.5 mV s^{-1} between −0.1 and −0.65 V in a 10 mM Tris buffer (pH 7.2) containing 1 M NaCl.

and leucomethylene blue forms. At potentials between −150 and −700 mV, i.e., where the DNA binder is in oxidized form, the intensity of this peak remains fairly constant. However, as the potential is driven between −700 and −1000 mV (Figure 7B), i.e., where the DNA binder is in reduced form, an increase in the peak intensity is observed. A similar increase has been observed previously in electrochemical melting assays where the labels Texas Red[26] and anthraquinone[27] were covalently bound to the DNA and is believed to be due to a reorientation of the immobilized dsDNA layer such that the reporter molecule is moved to a more favorable orientation relative to the substrate surface, increasing the SERS enhancement.

Reversible changes in the orientation of dsDNA at electrode surfaces of the type suggested here have been investigated by Rant[65−67] using fluorescence measurements, where fluorescence quenching results in a decrease in signal intensity when the label is re-oriented to a position closer to the metal surface. Meanwhile the second peak, centered at 1390 cm^{-1}, is present only in methylene blue and attenuates as the potential is driven negative in a way similar to that observed for the 1622 cm^{-1} peak assigned to the C═N stretch (Figure 7B).

When the methylene blue is reduced to leucomethylene blue, the 1622 cm^{-1} band no longer appears in the SERS spectrum. As the C═N band attenuates, it is replaced by a weak band at 1584 cm^{-1}, which is tentatively assigned as the C−N−C stretch of leucomethylene blue. Attenuation of the C═N stretch at 1622 cm^{-1} was used to extract electrochemical information about the methylene blue/leuco couple. A Nernst function was

dx.doi.org/10.1021/ja304663t | J. Am. Chem. Soc. 2012, 134, 14099−14107

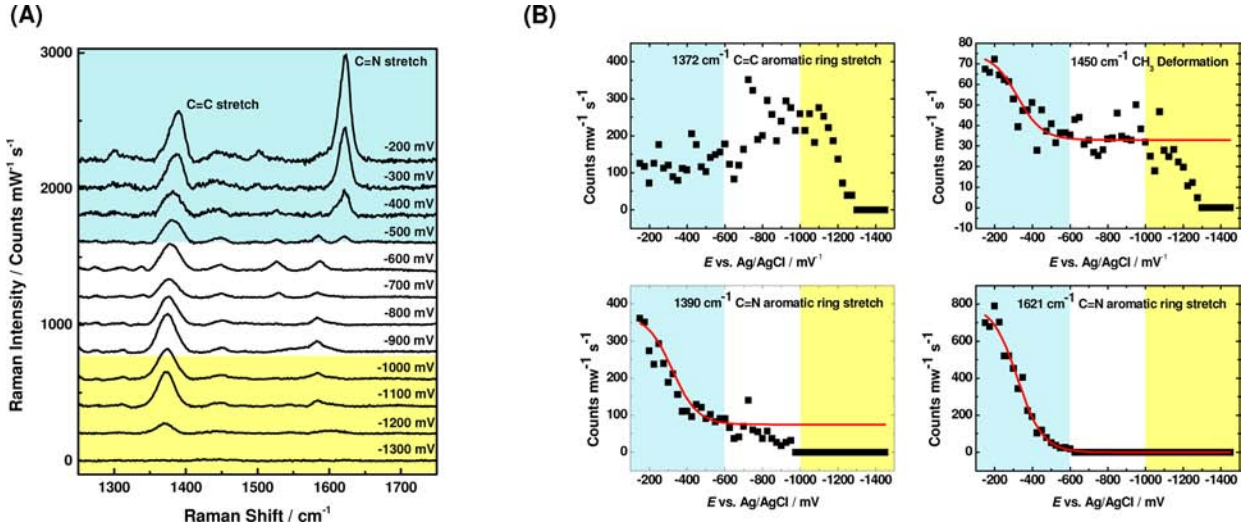

Figure 7. (A) Representative SERS spectra and (B) changes in peak height as a function of applied potential illustrating electrochemical reduction of dsDNA-bound methylene blue and subsequent electrochemical melting. The red lines are the Nernstian curves (see text for details). The potential was swept a scan rate of 0.05 mV s^{-1} in a 10 mM Tris buffer (pH 7.2) with 1 M NaCl. Spectra were acquired with a 2.7 mW 633 nm excitation laser and have been background subtracted and normalized with respect to laser power and accumulation time. Blue shading corresponds to methylene blue, colorless to leucomethylene blue, and yellow to dsDNA melting.

fitted to the attenuation of the band (red line in Figure 7B and Supporting Information) in order to determine the mid-peak potential of the methylene blue/leuco, using a method described in our previous work for the reduction of flavin at a silver substrate.[68] We found the the mid-peak potential for the methylene blue/leuco couple bound to the minor groove of the dsDNA to be −322 ± 8 mV vs Ag/AgCl (1 M NaCl, pH 7.2). Values of −250 mV vs SCE (pH 7)[69] and −310 mV vs Ag/AgCl (pH 7.4) have previously been reported for the methylene blue/leuco couple bound to dsDNA.[70] This represents a cathodic shift in potential relative to that observed for the couple when covalently attached to an immobilized DNA molecule, where values of −230 mV vs Ag/AgCl (pH 7)[71] and −215 mV vs Ag/AgCl (pH 7.4)[72] have been reported. This cathodic shift is consistent with close interaction of the methylene blue with the negatively charged dsDNA.

Full de-convolution of the methylene blue band at 1390 cm^{-1} was not possible, probably due to the presence of more than two overlapping peaks. Instead the Nernst function obtained from fitting the data at 1622 cm^{-1} (appropriately scaled for differences in intensity) was overlain on the data for the bands at 1390 and 1450 cm^{-1} (Figure 7B, red lines, and Supporting Information). The results show good agreement. We attribute the band at 1450 cm^{-1} to a CH_3 deformation of the methylene blue/leuco couple, and the data presented here are consistent with this assignment, because the attenuation, which is due to the loss of resonance upon reduction of methylene blue, is not as pronounced as would be expected if the band were strongly coupled with a molecular vibration directly linked to the π-to-π^* transition of the resonant chromophore.

While no longer resonant with the 633 nm excitation source, dsDNA-bound leucomethylene blue could still be detected with SERS and therefore used as a reporter molecule in a label-free SERS assay. The most intense band in leucomethylene blue is the C═C ring stretch, which is centered at 1372 cm^{-1} and the intensity of which was extracted by peak de-convolution as described in the Supporting Information. Upon driving the potential cathodic beyond −1000 mV vs Ag/AgCl, there is an irreversible loss in SERS intensity, which can be attributed to the electrochemically driven DNA denaturation. To demonstrate the utility of this approach, changes in the C═C stretch of leucomethylene blue as a function of applied potential were utilized to monitor electrochemically driven DNA denaturation of mutations in the CFTR gene (Figure 8). The results show

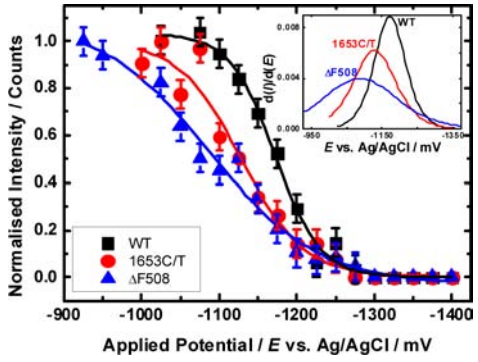

Figure 8. Discrimination of mutations in the CFTR gene utilizing label-free electrochemical melting. The variation of the peak intensity at 1372 cm^{-1} is plotted as a function of applied potential. In each case the potential was swept at 0.5 mV s^{-1} from an initial potential of −0.1 V in 10 mM Tris buffer (pH 7.2) containing 1 M NaCl. Spectra were acquired every 25 mV in static mode with a single 30 s acquisition. Sigmoidal curves were fitted to the data, and the first derivatives of these curves are shown inset.

that the single nucleotide polymorphism and a triplet deletion can be clearly distinguished from the fully complementary sequence in a label-free electrochemical melting experiment in which leucomethylene blue is used as the reporter molecule. The discrimination of mutations using this method can also be performed when the target is a PCR amplicon (Supporting Information Figure S5). Hybridization of the amplicon to the probe at the substrate surface occurs without the need for prior purification, highlighting the feasibility of this approach for DNA testing.

dx.doi.org/10.1021/ja304663t | J. Am. Chem. Soc. 2012, 134, 14099−14107

CONCLUSIONS

The discrimination of mutations in the CFTR gene without the need to synthetically attach a dye label to the target strand has been demonstrated. SER(R)S is used to monitor electrochemically driven DNA denaturation from the spectra of dsDNA-exclusive binding agents. Since electrochemical melting discriminates between sequences on the basis of the stability of the duplex, we anticipate that the label-free method described here can be applied to a wide range of targets of interest, and thus demonstrates significant future potential for integration into a point-of-care device. The correct choice of binding agent is critical to the success of a label-free SERS discrimination assay. Factors such as resonance with the pump laser, orientation relative to the SERS surface, and degree of dsDNA binding selectivity (with respect to ssDNA) must all be considered.

ASSOCIATED CONTENT

Supporting Information

Details of the peak de-convolution method, extraction of mid-peak potentials for methylene blue bound to dsDNA, and discrimination of mutations from PCR products. This material is available free of charge via the Internet at http://pubs.acs.org.

AUTHOR INFORMATION

Corresponding Author

pnb@soton.ac.uk

Notes

The authors declare no competing financial interest.

ACKNOWLEDGMENTS

This work was supported by the UK EPSRC via a Doctoral Prize Award (R.P.J.).

REFERENCES

(1) Kerem, B.; Rommens, J.; Buchanan, J.; Markiewicz, D.; Cox, T.; Chakravarti, A.; Buchwald, M.; Tsui, L. *Science* **1989**, *245*, 1073.
(2) Goldstein, D. B.; Tate, S. K.; Sisodiya, S. M. *Nat. Rev. Genet.* **2003**, *4*, 937.
(3) Drummond, T. G.; Hill, M. G.; Barton, J. K. *Nat. Biotechnol.* **2003**, *21*, 1192.
(4) Star, A.; Tu, E.; Niemann, J.; Gabriel, J.-C. P.; Joiner, C. S.; Valcke, C. *Proc. Natl. Acad. Sci. U.S.A.* **2006**, *103*, 921.
(5) Sorgenfrei, S.; Chiu, C.-y.; Gonzalez, R. L.; Yu, Y.-J.; Kim, P.; Nuckolls, C.; Shepard, K. L. *Nat. Nanotechnol.* **2011**, *6*, 126.
(6) Peng, H.-I.; Strohsahl, C. M.; Leach, K. E.; Krauss, T. D.; Miller, B. L. *ACS Nano* **2009**, *3*, 2265.
(7) Ho, H.-A.; Boissinot, M.; Bergeron, M. G.; Corbeil, G.; Doré, K.; Boudreau, D.; Leclerc, M. *Angew. Chem., Int. Ed.* **2002**, *41*, 1548.
(8) Nilsson, K. P. R.; Inganas, O. *Nat. Mater.* **2003**, *2*, 419.
(9) Wang, S.; Gaylord, B. S.; Bazan, G. C. *J. Am. Chem. Soc.* **2004**, *126*, 5446.
(10) McKendry, R.; Zhang, J.; Arntz, Y.; Strunz, T.; Hegner, M.; Lang, H. P.; Baller, M. K.; Certa, U.; Meyer, E.; Güntherodt, H.-J.; Gerber, C. *Proc. Natl. Acad. Sci. U.S.A.* **2002**, *99*, 9783.
(11) Wang, J.; Jiang, M.; Palecek, E. *Bioelectrochem. Bioenerg.* **1999**, *48*, 477.
(12) Yao, X.; Li, X.; Toledo, F.; Zurita-Lopez, C.; Gutova, M.; Momand, J.; Zhou, F. *Anal. Biochem.* **2006**, *354*, 220.
(13) Luan, Q.; Xue, Y.; Yao, X. *Sens. Actuators B-Chem.* **2010**, *147*, 561.
(14) Barhoumi, A.; Halas, N. J. *J. Am. Chem. Soc.* **2010**, *132*, 12792.
(15) Paleček, E.; Bartošík, M. *Chem. Rev.* **2012**, in press.
(16) Hvastkovs, E. G.; Buttry, D. A. *Analyst* **2010**, *135*, 1817.
(17) Keighley, S. D.; Estrela, P.; Li, P.; Migliorato, P. *Biosens. Bioelectron.* **2008**, *24*, 906.
(18) Li, A.; Yang, F.; Ma, Y.; Yang, X. *Biosens. Bioelectron.* **2007**, *22*, 1716.
(19) Kafka, J.; Pänke, O.; Abendroth, B.; Lisdat, F. *Electrochim. Acta* **2008**, *53*, 7467.
(20) Nasef, H.; Beni, V.; O'Sullivan, C. K. *Anal. Methods* **2010**, *2*, 1461.
(21) Sosnowski, R. G.; Tu, E.; Butler, W. F.; O'Connell, J. P.; Heller, M. J. *Proc. Natl. Acad. Sci. U.S.A.* **1997**, *94*, 1119.
(22) Heaton, R. J.; Peterson, A. W.; Georgiadis, R. M. *Proc. Natl. Acad. Sci. U.S.A.* **2001**, *98*, 3701.
(23) Papadopoulou, E.; Bell, S. E. J. *Angew. Chem., Int. Ed.* **2011**, *50*, 9058.
(24) Corrigan, D. K.; Gale, N.; Brown, T.; Bartlett, P. N. *Angew. Chem.* **2010**, *122*, 6053.
(25) Johnson, R. P.; Gao, R.; Brown, T.; Bartlett, P. N. *Bioelectrochemistry* **2012**, *85*, 7.
(26) Mahajan, S.; Richardson, J.; Brown, T.; Bartlett, P. N. *J. Am. Chem. Soc.* **2008**, *130*, 15589.
(27) Mahajan, S.; Richardson, J.; Gaied, N. B.; Zhao, Z.; Brown, T.; Bartlett, P. N. *Electroanalysis* **2009**, *21*, 2190.
(28) Johnson, R. P.; Richardson, J. A.; Brown, T.; Bartlett, P. N. *Langmuir* **2012**, *28*, 5464.
(29) Heaton, R. J.; Peterson, A. W.; Georgiadis, R. M. *Proc. Natl. Acad. Sci. U.S.A.* **2001**, *98*, 3701.
(30) Herne, T. M.; Tarlov, M. J. *J. Am. Chem. Soc.* **1997**, *119*, 8916.
(31) Erts, D.; Polyakov, B.; Olin, H.; Tuite, E. *J. Phys. Chem. B* **2003**, *107*, 3591.
(32) Lee, C.-Y.; Gong, P.; Harbers, G. M.; Grainger, D. W.; Castner, D. G.; Gamble, L. J. *Anal. Chem.* **2006**, *78*, 3316.
(33) Li, Z.; Jin, R.; Mirkin, C. A.; Letsinger, R. L. *Nucleic Acids Res.* **2002**, *30*, 1558.
(34) Sakata, T.; Maruyama, S.; Ueda, A.; Otsuka, H.; Miyahara, Y. *Langmuir* **2007**, *23*, 2269.
(35) Mahajan, S.; Richardson, J.; Brown, T.; Bartlett, P. N. *J. Am. Chem. Soc.* **2008**, *130*, 15589.
(36) Suh, D.; Chaires, J. B. *Biorg. Med. Chem.* **1995**, *3*, 723.
(37) Gao, X.; Davies, J. P.; Weaver, M. J. *J. Phys. Chem.* **1990**, *94*, 6858.
(38) Moskovits, M.; Suh, J. S. *J. Phys. Chem.* **1984**, *88*, 5526.
(39) Nafisi, S.; Saboury, A. A.; Keramat, N.; Neault, J.-F.; Tajmir-Riahi, H.-A. *J. Mol. Struct.* **2007**, *827*, 35.
(40) Njoh, K. L.; Patterson, L. H.; Zloh, M.; Wiltshire, M.; Fisher, J.; Chappell, S.; Ameer-Beg, S.; Bai, Y.; Matthews, D.; Errington, R. J.; Smith, P. J. *Cytometry Part A* **2006**, *69A*, 805.
(41) Gilbert, D. E.; Feigon, J. *Curr. Opin. Struct. Biol* **1991**, *1*, 439.
(42) Neidle, S.; Pearl, L. H.; Skelly, J. V. *Biochem. J.* **1987**, *243*, 1.
(43) Rohs, R.; Bloch, I.; Sklenar, H.; Shakked, Z. *Nucleic Acids Res.* **2005**, *33*, 7048.
(44) Tuite, E.; Norden, B. *J. Am. Chem. Soc.* **1994**, *116*, 7548.
(45) Virant-Klun, I.; Tomazevic, T.; Meden-Vrtovec, H. *J. Assist. Reprod. Genet.* **2002**, *19*, 319.
(46) Kaiser, W.; Rant, U. *J. Am. Chem. Soc.* **2010**, *132*, 7935.
(47) Mahajan, S.; Baumberg, J. J.; Russell, A. E.; Bartlett, P. N. *Phys. Chem. Chem. Phys.* **2007**, *9*, 6016.
(48) Zimmerman, F.; Hossenfelder, B.; Panitz, J. C.; Wokaun, A. *J. Phys. Chem.* **1994**, *98*, 12796.
(49) Lyles, M. B.; Cameron, I. L. *Biophys. Chem.* **2002**, *96*, 53.
(50) Pjura, P. E.; Grzeskowiak, K.; Dickerson, R. E. *J. Mol. Biol.* **1987**, *197*, 257.
(51) Kubista, M.; Aakerman, B.; Norden, B. *Biochemistry* **1987**, *26*, 4545.
(52) Wilson, W. D.; Tanious, F. A.; Barton, H. J.; Jones, R. L.; Strekowski, L.; Boykin, D. W. *J. Am. Chem. Soc.* **1989**, *111*, 5008.
(53) Wilson, W. D.; Tanious, F. A.; Barton, H. J.; Jones, R. L.; Fox, K.; Wydra, R. L.; Strekowski, L. *Biochemistry* **1990**, *29*, 8452.
(54) Kneipp, K.; Kneipp, H.; Rentsch, M. *J. Mol. Struct.* **1987**, *156*, 331.

(55) Zimmermann, F.; Zimmermann, B.; Panitz, J. C.; Wokaun, A. *J. Raman Spectrosc.* **1995**, *26*, 435.
(56) Tognalli, N. G.; Fainstein, A.; Vericat, C.; Vela, M. E.; Salvarezza, R. C. *J. Phys. Chem. B* **2005**, *110*, 354.
(57) Erdem, A.; Kerman, K.; Meric, B.; Ozsoz, M. *Electroanalysis* **2001**, *13*, 219.
(58) Yang, W.; Ozsoz, M.; Hibbert, D. B.; Gooding, J. J. *Electroanalysis* **2002**, *14*, 1299.
(59) Kerman, K.; Ozkan, D.; Kara, P.; Meric, B.; Gooding, J. J.; Ozsoz, M. *Anal. Chim. Acta* **2002**, *462*, 39.
(60) Xiao, G.-N.; Man, S.-Q. *Chem. Phys. Lett.* **2007**, *447*, 305.
(61) Nicolai, S. H. A.; Rubim, J. C. *Langmuir* **2003**, *19*, 4291.
(62) Hutchinson, K.; Hester, R. E.; Albery, W. J.; Hillman, A. R. *J. Chem. Soc., Faraday Trans* **1984**, *80*, 2053.
(63) Gorodetsky, A. A.; Buzzeo, M. C.; Barton, J. K. *Bioconjugate Chem.* **2008**, *19*, 2285.
(64) Boon, E. M.; Barton, J. K.; Bhagat, V.; Nersissian, M.; Wang, W.; Hill, M. G. *Langmuir* **2003**, *19*, 9255.
(65) Rant, U.; Arinaga, K.; Fujita, S.; Yokoyama, N.; Abstreiter, G.; Tornow, M. *Nano Lett.* **2004**, *4*, 2441.
(66) Rant, U.; Arinaga, K.; Fujita, S.; Yokoyama, N.; Abstreiter, G.; Tornow, M. *Org. Biomol. Chem.* **2006**, *4*, 3448.
(67) Rant, U.; Arinaga, K.; Tornow, M.; Kim, Y. W.; Netz, R. R.; Fujita, S.; Yokoyama, N.; Abstreiter, G. *Biophys. J.* **2006**, *90*, 3666.
(68) Abdelsalam, M.; Bartlett, P. N.; Russell, A. E.; Baumberg, J. J.; Calvo, E. J.; Tognalli, N. s. G.; Fainstein, A. *Langmuir* **2008**, *24*, 7018.
(69) Kelley, S. O.; Barton, J. K.; Jackson, N. M.; Hill, M. G. *Bioconjugate Chem.* **1997**, *8*, 31.
(70) Zhang, D.; Peng, Y.; Qi, H.; Gao, Q.; Zhang, C. *Biosens. Bioelectron.* **2010**, *25*, 1088.
(71) Uzawa, T.; Cheng, R. R.; White, R. J.; Makarov, D. E.; Plaxco, K. W. *J. Am. Chem. Soc.* **2010**, *132*, 16120.
(72) Nasef, H.; Beni, V.; O'Sullivan, C. K. *J. Electroanal. Chem.* **2011**, *662*, 322.

■ NOTE ADDED AFTER ASAP PUBLICATION

This paper was published ASAP on August 9, 2012. Figures 6 and 8 have been updated. The revised version was posted on August 15, 2012.